



Preparation, Characterization, and Electrocatalytic Properties of mvRuO/RuCN and RP Hybrid Film-Modified Electrodes

Shen-Ming Chen^z and Sheh-Hung Hsueh

Department of Chemical Engineering, National Taipei University of Technology, Taipei, Taiwan 106, China

Ruthenium oxide/ruthenocyanide (ruthenium oxide/hexacyanoruthenate, or mvRuO/RuCN) and iron(III) ruthenocyanide (ruthenium purple, or RP) hybrid films have been prepared using consecutive cyclic voltammetry, and the deposition process and the films' electrocatalytic properties in electrolytes containing Rb⁺ and Cs⁺ have been investigated. The hybrid ruthenium oxide/ruthenocyanide and RP films showed four obvious and separated redox couples with formal potentials between -0.2 and 1.0 V in monovalent cation aqueous solutions of RbNO₃ or CsNO₃. The cyclic voltammograms recorded the deposition of the hybrid films directly from the mixing of Ru³⁺, Fe³⁺, and Ru(CN)₆⁴⁻ ions in aqueous Rb⁺ or Cs⁺ cation solutions. An electrochemical quartz crystal microbalance and cyclic voltammetry were used to study the growth mechanism of the hybrid films. The electrochemical properties of the films indicate that the redox process was confined to the immobilized and mixed ruthenium oxide/ruthenocyanide and RP films. The electrocatalytic reduction properties of SO₅²⁻ and S₂O₈²⁻ by the hybrid films were also determined, as well as the electrocatalytic properties of dopamine and epinephrine. The electrocatalytic reactions of the hybrid films were investigated using the rotating ring-disk electrode method.

© 2004 The Electrochemical Society. [DOI: 10.1149/1.1666189] All rights reserved.

Manuscript submitted July 7, 2003; revised manuscript received October 23, 2003. Available electronically March 3, 2004.

Iron ruthenocyanide (ruthenium purple, or RP) and ruthenium oxide/ruthenocyanide (ruthenium oxide/hexacyanoruthenate or mvRuO/RuCN) are the ruthenium analogs of iron hexacyanoferrate. Metal hexacyanoferrates and metal ruthenocyanides show interesting redox chemistry that is accompanied by changes in their electrochromic, ion exchange, and electrocatalytic properties. Metal hexacyanoferrate¹⁻⁶ chemically modified film electrodes show interesting electrochemical properties. They are used in both chemistry and in material science, in such areas as electroanalysis, chemical sensing, and electrocatalysis,⁷⁻¹⁵ in studies on interfacial charges, electrochromicity, in the study of ion-exchange and electron-transfer processes,¹⁶⁻¹⁸ and in research on the chemical composition of surface films.¹⁹

An RP film can be deposited onto a working electrode using a two-step procedure,^{20,21} and an mvRuO/RuCN film can be deposited onto a working electrode by cycling the potential between 0.5 and 1.0 V using Ru(CN)₆²⁻ in an aqueous 0.5 M KCl solution at pH 2.²²⁻²⁷ To realize practical applications of RP and ruthenium oxide/ruthenocyanide film-modified electrodes for ion sensor applications, the deposition processes of these films must be fully characterized.

An important and interesting possibility is a modified hybrid electrode containing RP and mvRuO/RuCN films that have different properties, which can be used to convert reactants to selected products. Hybrid films are highly relevant to contemporary material science, and a hybrid RP and mvRuO/RuCN film is a member of this interesting class of materials.

This paper discusses the successful preparation of hybrid films of iron ruthenocyanide and ruthenium oxide/ruthenocyanide in aqueous Rb⁺ and Cs⁺ electrolytic solutions. These show good stability, as well as well-defined redox couples and electrocatalytic properties. No previous discussion has occurred in the literature on the preparation of RP and mvRuO/RuCN hybrid films, although a few reports concerning their electrocatalytic properties²⁸ and electrochemical quartz crystal microbalance (EQCM) measurements²⁹ have been cited.

The fabrication of a chemically modified film electrode is easily controlled using consecutive cyclic voltammetry (CV), because in this synthetic method, an increase in the peak current of the film induces the appropriate redox couple of the modified film. Results of

the electrocatalytic activity measurements are applicable to analytical applications and to the electrochemical oxidation of low electroactive compounds.

This paper discusses the first successful preparation of a hybrid film of iron ruthenocyanide and ruthenium oxide/ruthenocyanide in aqueous Rb⁺ and Cs⁺ electrolytic solutions and their resulting electrocatalytic properties. The paper also discusses the electrocatalytic properties and EQCM measurements made during the deposition and ion-exchange processes of the RP and mvRuO/RuCN hybrid film. Simultaneous CV and microgravimetry using an EQCM can continuously detect *in situ* the surface mass change on an electrode in an experimental solution. This technique is useful for elucidating the growth mechanism and electrochemical properties of RP and mvRuO/RuCN films, as well as their hybrid films. The electrocatalytic reduction of SO₅²⁻ and S₂O₈²⁻ by an RP and mvRuO/RuCN hybrid film was observed, as well as the reversible electrocatalysis of dopamine and epinephrine. The analytical methods used are established techniques and are important for the determination of these analytes. Dopamine and epinephrine are important neurotransmitters in the mammalian central nervous system, and therefore the development of electrochemical methods that can be used to monitor these compounds is important. The electrocatalytic reduction of peroxosulfate and persulfate is of interest for environmental applications, and the electrocatalytic oxidation of dopamine and epinephrine is of interest for biomedical applications. The electrocatalytic oxidation of dopamine was active, and the products of the oxidation of dopamine could be electrocatalytically reduced. The electrocatalytic reactions of dopamine and epinephrine by an RP and mvRuO/RuCN hybrid film were investigated using the rotating ring-disk electrode (RRDE) method.

Experimental

Electrochemistry was performed using a Bioanalytical Systems model CV-50W and CH Instruments CHI-400 and CHI-750 potentiostats. CV was conducted using a three-electrode cell in which a BAS glassy carbon (GC) electrode, a platinum electrode, and a tin dioxide electrode were used as the working electrodes. The GC electrode was polished with 50 nm alumina on Buehler felt pads and then ultrasonically cleaned for 1 min. The auxiliary compartment contained a platinum wire, which was separated from the rest of the compartment by a medium-sized glass frit. All cell potentials were measured using either a Ag|AgCl|KCl (saturated solution) reference electrode or a Hg|Hg₂Cl₂|KCl (saturated solution) reference electrode.

^z E-mail: smchen78@ms15.hinet.net

The working electrode for the EQCM measurements was an 8 MHz AT-cut quartz crystal with gold electrodes. The diameter of the quartz crystal was 13.7 mm and the gold electrode diameter was 5 mm. The spectroelectrochemical cell consisted of a 1 mm cuvette, a 100-mesh platinum gauze used as a working electrode, a platinum wire used as an auxiliary electrode, and an Ag|AgCl reference electrode.

RRDE experiments were performed using a Pine Instruments Co. electrode in conjunction with a CH Instruments CHI-750 potentiostat connected to a model AFMSRX analytical rotator. The rotating disk electrode (RDE), purchased from the Pine Instruments Co., consisted of a GC disk electrode and a GC (or platinum) ring electrode.

UV-visible spectra were measured using a Hitachi model U-3300 spectrophotometer.

The ion chromatograph used in the experiments was a Dionex Instruments ion chromatograph model DX-100, which consisted of a pump, a conductivity detector, an electrochemical detector, and a syringe loading system with a 25 μ L sample loop. The columns used throughout were an IonPac AG4A guard column, an IonPac AS4A analytical column, and an anion self-regenerating suppressor column. All measurements were conducted at room temperature.

All chemicals used were of analytical grade. The aqueous solutions were prepared using doubly distilled deionized water, and the solutions were deoxygenated by purging with prepurified nitrogen gas.

The electrochemical formation of the hybrid iron ruthenocyanide and ruthenium oxide/ruthenocyanide films was performed by continuous cycling of the potential of the working electrode in a defined potential range in a suitable aqueous solution containing Ru^{3+} , Fe^{3+} , and $\text{Ru}(\text{CN})_6^{4-}$ ions. Typical electrochemical formation of hybrid RP and mvRuO/RuCN films was performed by repetitive CV on cycling the potential of the working electrode in a defined potential range in an aqueous Rb^+ or Cs^+ supporting electrolyte solution containing $\text{K}_4\text{Ru}(\text{CN})_6$ with Ru^{3+} (with the balancing anion being chloride or nitrate).

Results and Discussion

Hybrid RP and mvRuO/RuCN film deposition in aqueous RbNO_3 and CsNO_3 solutions.—The electrochemical formation of hybrid iron ruthenocyanide and ruthenium oxide/ruthenocyanide films on a GC electrode was carried out using consecutive CV in aqueous RbNO_3 and CsNO_3 solutions.

The hybrid RP and mvRuO/RuCN film showed four redox couples with formal potentials at -0.05 , 0.26 , 0.73 , and 0.94 V, respectively, in aqueous monovalent cation RbNO_3 solutions (Fig. 1A). Figure 1B shows the consecutive CVs of the hybrid RP and mvRuO/RuCN film showing the four redox couples with formal potentials at 0.03 , 0.28 , 0.64 , and 0.90 V in aqueous CsNO_3 solutions. The reason for choosing cesium and rubidium as the electrolyte solution salts is that the films exhibited four clear redox couples with cesium or rubidium electrolytes, but with lithium, potassium, or sodium salt electrolytes the four redox couples were not well separated or did not exhibit a well-defined shape.

The results show the successful formation of a hybrid RP and mvRuO/RuCN film and demonstrate that the voltammetric properties of the hybrid RP and mvRuO/RuCN film depend on the monovalent cation (Rb^+ or Cs^+) of the electrolyte. The experimental results also show that the hybrid RP and mvRuO/RuCN films can be formed directly from the mixing of Fe^{3+} , Ru^{3+} , and $\text{Ru}(\text{CN})_6^{4-}$ ions by consecutive CV using Rb^+ and Cs^+ cations as the electrolyte solution and give the four separate redox couples (see Fig. 1 and Table I).

Figure 2A shows that a hybrid RP and mvRuO/RuCN film was obtained on a GC electrode from the 0.2 M aqueous RbNO_3 solution at pH 2.0 and shows four chemically reversible redox couples for various scan rates. The inset of Fig. 2A shows a plot of the anodic peak current, I_{pa} , vs. scan rate at a potential of 0.15 V, illustrating a

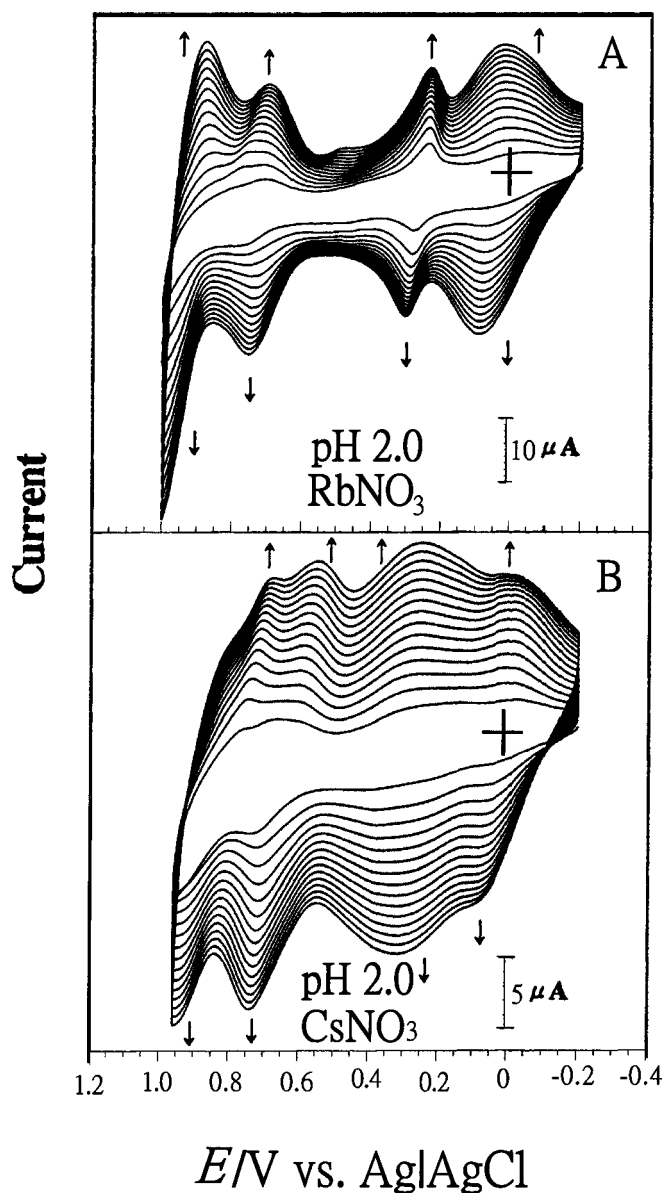


Figure 1. Repetitive CVs of a GC electrode modified with a hybrid ruthenium oxide/ruthenocyanide and iron(III) ruthenocyanide film synthesized from 2×10^{-3} M $\text{Ru}(\text{CN})_6^{4-}$ added to aqueous 1×10^{-3} M Ru^{3+} and 1×10^{-3} M Fe^{3+} mixed in a pH 2.0 aqueous solution of: (A) 0.2 M RbNO_3 and (B) 0.2 M CsNO_3 . Scan rate 0.1 V/s.

close linear dependence of I_{pa} on the scan rate, with the ratio of the anodic to cathodic peak current, I_{pa}/I_{pc} , equal to unity.

Table I. The electrochemical properties of RP, mvRuO/RuCN, and RP and mvRuO/RuCN hybrid films.

Film/electrolyte	RbNO_3 (V)	CsNO_3 (V)	pH
Ironruthenocyanide	0.30	0.34	2.0
Ruthenium oxide/ruthenocyanide	0.03	0.06	2.0
RP and mvRuO/RuCN	0.68	0.70	2.0
	0.92	+0.96	
	0.06	0.04	
	0.26	0.28	
	0.72	0.64	
	0.92	0.86	

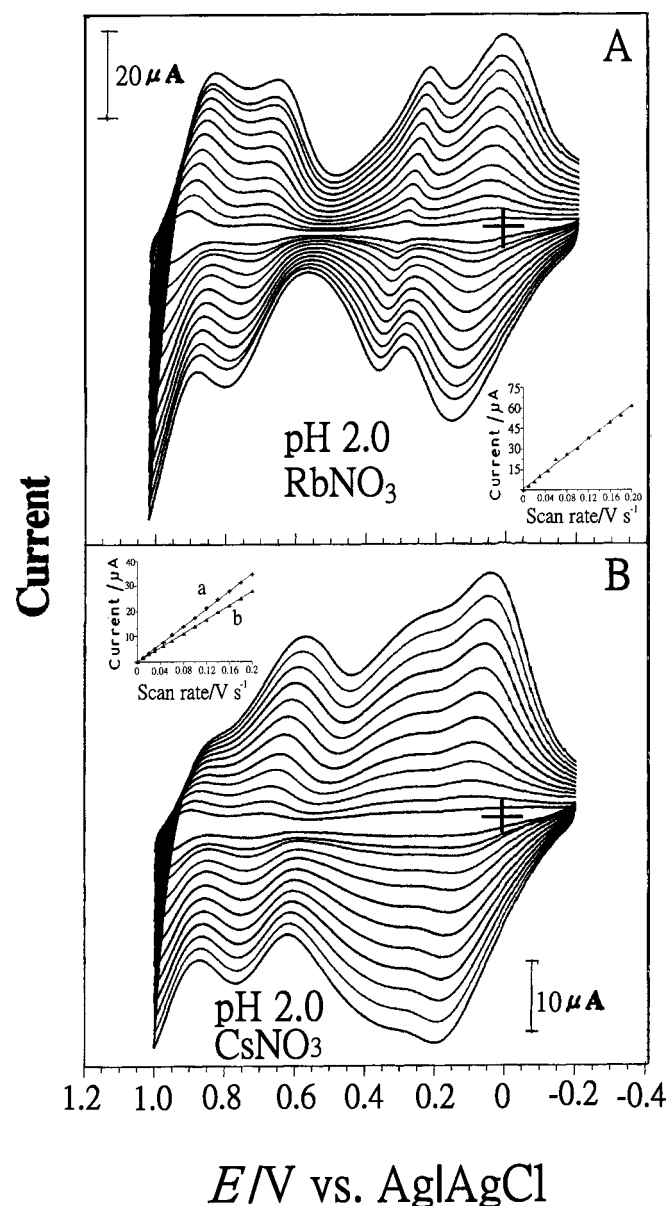


Figure 2. (A) CVs of a GC electrode modified with a hybrid RP and mvRuO/RuCN film in an aqueous solution at pH 2.0 of (A) 0.2 M RbNO₃ and (B) 0.2 M CsNO₃ for scan rates of (a) 0.01, (b) 0.02, (c) 0.03, (d) 0.045, (e) 0.06, (f) 0.08, (g) 0.10, (h) 0.12, (i) 0.14, (j) 0.16, (k) 0.18, and (l) 0.20 V/s. Inset 2A: Plot of the anodic peak current (at a potential of 0.15 V) vs. scan rate. Inset 2B: Plot of the cathodic peak current (at a potential of 0.05 V) and (b) anodic peak current vs. scan rate at a potential of about 0.40 V.

Figure 2B shows that a hybrid RP and mvRuO/RuCN film was obtained on a GC electrode from the 0.2 M aqueous CsNO₃ solution at pH 2.0 and shows three chemically reversible redox couples between potentials of -0.2 and 0.9 V for various scan rates. The inset of Fig. 2B shows a plot of: (a) the cathodic peak current at a potential of 0.05 V and (b) the anodic peak current at about 0.40 V vs. scan rate, illustrating a close linear dependence of I_p on the scan rate, and that I_{pa}/I_{pc} was close to unity. The behavior shown in Fig. 2A and B is consistent with a surface-type behavior, a reversible electron-transfer process at low scan rates. The peak current and scan rate are related by the following equation^{30,31}

$$I_p = n^2 F^2 \nu A \Gamma_0 / 4MRT \quad [1]$$

where Γ_0 (g/cm²), ν , A , I_p , and M (g/mol) represent the surface coverage concentration, the scan rate, the electrode area, the peak current, and the effective molar mass, respectively. This result indicates that the redox process was confined to the surface of the hybrid RP and mvRuO/RuCN film on the GC electrode, confirming the immobilized state of the hybrid RP and mvRuO/RuCN film.^{30,31} The four redox couples are proposed to arise from the [Ru^{II}-O]/[Ru^{II}(CN)₆]/[Ru^{III}-O]/[Ru^{II}(CN)₆], [Fe^{II}-NC-Ru^{III}]/[Fe^{III}-NC-Ru^{III}], [Ru^{III}-O]/[Ru^{II}(CN)₆]/[Ru^{III}-O]/[Ru^{III}(CN)₆], and [Ru^{III}-O]/[Ru^{III}(CN)₆]/[Ru^{IV}-O]/[Ru^{III}(CN)₆] processes in passing from the negative to the positive potential regions.

Figure 3A(a) shows RP formation CVs that exhibit one redox couple with a formal potential at about $E^{o'} = 0.30$ V (vs. Ag|AgCl) in an aqueous 0.2 M RbNO₃ solution at pH 2.0. Figure 3A(b) shows the CVs of mvRuO/RuCN film formation, which exhibit three redox couples with formal potentials at about $E^{o'} = 0.03$, 0.68 , and 0.92 V (vs. Ag|AgCl), respectively, in an aqueous 0.2 M RbNO₃ solution at pH 2.0. The CVs of RP and mvRuO/RuCN film formation exhibit four redox couples with formal potentials at about $E^{o'} = 0.06$, 0.26 , 0.72 , and 0.92 V (vs. Ag|AgCl), respectively, in an aqueous 0.2 M RbNO₃ solution at pH 2.0.

Figure 3B(a) shows RP formation CVs that exhibit one redox couple with a formal potential at about $E^{o'} = 0.34$ V (vs. Ag|AgCl) in an aqueous 0.2 M CsNO₃ solution at pH 2.0. Figure 3B(b) shows the CVs of mvRuO/RuCN film formation, which exhibit three redox couples with formal potentials at about $E^{o'} = 0.06$, 0.70 , and 0.96 V (vs. Ag|AgCl), respectively, in an aqueous 0.2 M CsNO₃ solution at pH 2.0. The CVs of RP and mvRuO/RuCN film formation show four redox couples with formal potentials at about $E^{o'} = 0.04$, 0.28 , 0.64 , and 0.86 V (vs. Ag|AgCl), respectively, in an aqueous 0.2 M CsNO₃ solution at pH 2.0 (Table I).

RP, mvRuO/RuCN, and RP and mvRuO/RuCN hybrid film deposition and in situ EQCM measurements.—We successfully grew RP, mvRuO/RuCN, and RP and mvRuO/RuCN hybrid films on gold electrodes from an aqueous 0.2 M RbNO₃ solution at pH 2.0. The CVs are shown in Fig. 4A, with Fig. 4B showing the growth of the RP film on a gold electrode and the resulting change in EQCM frequency. The RP film obtained from the aqueous 0.2 M RbNO₃ solution at pH 2.0 showed a single redox couple occurring between potentials of -0.2 and 0.6 V, with the formal potential being at approximately 0.3 V (vs. Ag|AgCl). Figure 4B shows the EQCM frequency change recorded during the first ten cycles of the consecutive CV. The voltammetric peak current in Fig. 4A and the frequency decrease (or mass increase) in Fig. 4B are consistent with the growth of an RP film on the gold electrode. The EQCM results show that the deposition of the RP film occurred between the potential range 0.2 and -0.2 V (vs. Ag|AgCl). This potential range is the region where [Fe^{II}-NC-Ru^{II}] species form and deposit on the electrode surface.^{15,32-34}

In the EQCM experiments, the change in mass at the quartz crystal was calculated from the change in the measurement frequency using the Sauerbrey equation^{35,36}

$$\text{Mass change } (\Delta m) = (-1/2)(f_0^{-2})(\Delta f)A(k\rho)^{1/2} \quad [2]$$

where A is the area of the gold disk coated onto the quartz crystal, ρ is the density of the crystal, k is the shear modulus of the crystal, Δf is the measured frequency change, and f_0 is the oscillation frequency of the crystal. A frequency change of 1 Hz is equivalent to a change of 1.4 ng in mass. During the first CV scan, approximately 1890 ng/cm² of RP was deposited on the gold electrode. Approximately 9450 ng/cm² of RP was deposited on the gold electrode after ten CV scans.

We also successfully grew mvRuO/RuCN on a gold electrode from an aqueous 0.2 M RbNO₃ solution at pH 2.0. The CVs are shown in Fig. 5A, with Fig. 5B showing the growth of the mvRuO/

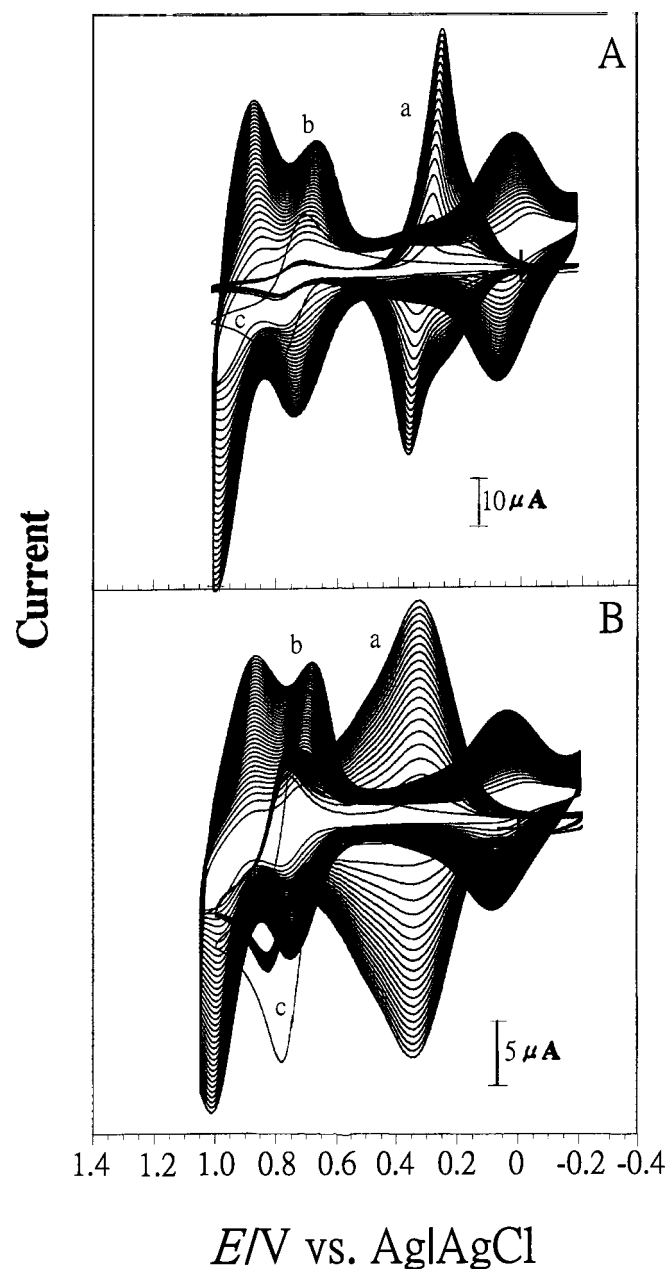


Figure 3. Repetitive CVs of a GC electrode modified with (a) an iron(III) ruthenocyanide film synthesized from 1×10^{-3} M Fe^{3+} and 2×10^{-3} M $\text{Ru}(\text{CN})_6^{4-}$, (b) a ruthenium oxide/ruthenocyanide film synthesized from 1×10^{-3} M Fe^{3+} and 2×10^{-3} M $\text{Ru}(\text{CN})_6^{4-}$, and (c) a film synthesized from 2×10^{-3} M $\text{Ru}(\text{CN})_6^{4-}$ in a pH 2.0 aqueous solution of (A) 0.2 M RbNO_3 and (B) 0.2 M CsNO_3 . Scan rate 0.1 V/s.

RuCN film on the gold electrode and the resulting change in the EQCM frequency. The mvRuO/RuCN film obtained from the aqueous 0.2 M RbNO_3 solution at pH 2.0 showed three redox couples occurring between potentials of -0.2 and 1.0 V, with the formal potentials being at approximately 0.03, 0.68, and 0.92 V (vs. Ag|AgCl). Figure 5B shows the EQCM frequency change recorded during the first seven cycles of the consecutive CV. The EQCM results show that the deposition of the film occurred between the potential range of 0.85 and 1.0 V (vs. Ag|AgCl). This potential range is where $[\text{Ru}^{\text{IV}}\text{-O}]/[\text{Ru}^{\text{III}}(\text{CN})_6]$ species form and deposit on the electrode surface.

The change in mass at the quartz crystal was calculated from the change in the measurement frequency using the Sauerbrey

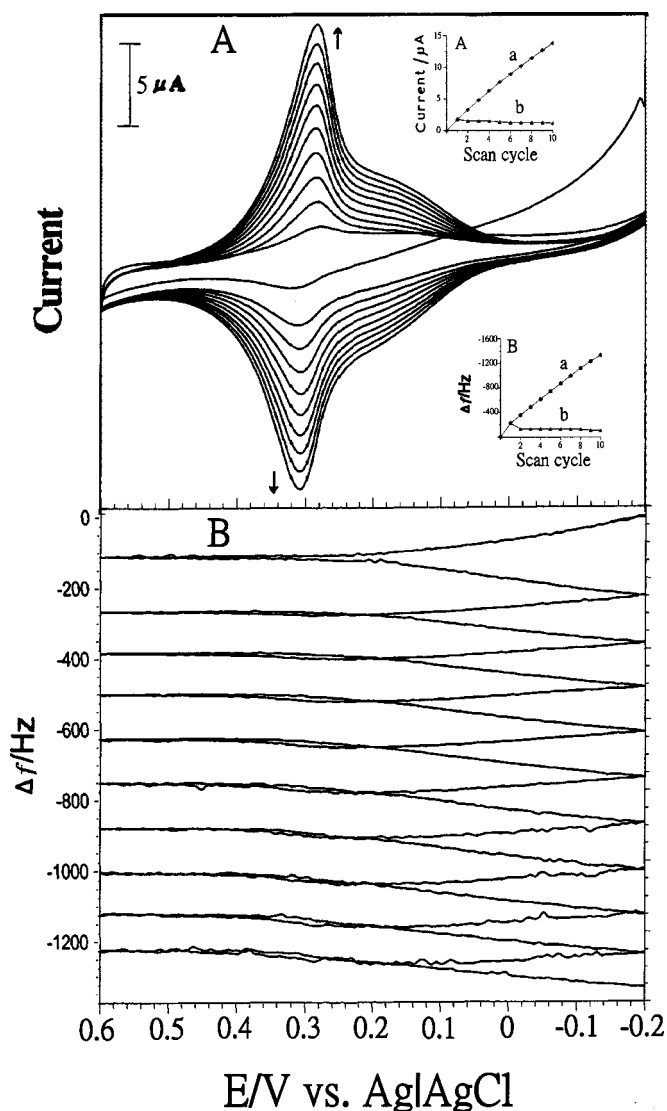


Figure 4. (A) Consecutive CVs of a gold electrode modified with an iron ruthenocyanide film synthesized from 1×10^{-3} M $\text{Ru}(\text{CN})_6^{4-}$ and added 2×10^{-4} M Fe^{3+} in an aqueous 0.2 M RbNO_3 solution at pH 2.0. Scan rate 0.02 V/s. (B) Change in EQCM frequency recorded concurrently with the consecutive CVs of Fig. 4A. Inset 4A: Plot of (a) cathodic peak current vs. scan cycle and (b) cathodic peak current change during a single scan cycle vs. scan cycle. Inset 4B: Plot of (a) total frequency change vs. scan cycle and (b) frequency change during a single scan vs. scan cycle.

equation.^{35,36} During the first CV scan, approximately 725 ng/cm^2 of mvRuO/RuCN was deposited on the gold electrode. Approximately 3808 ng/cm^2 of mvRuO/RuCN was deposited on the gold electrode after seven CV scans (see Fig. 5).

Successful growth of the RP and mvRuO/RuCN hybrid film on a gold electrode surface was achieved using an aqueous 0.2 M RbNO_3 solution at pH 2.0. Figure 6A shows the CVs of the RP and mvRuO/RuCN hybrid film deposition from an aqueous 0.2 M RbNO_3 solution at pH 2.0.

Figure 6 shows the growth of the RP and mvRuO/RuCN hybrid film and the resulting change in frequency in the EQCM measurements on a gold electrode in an aqueous 0.2 M RbNO_3 solution at pH 2.0. The film obtained from the aqueous 0.2 M RbNO_3 solution at pH 2.0 showed four redox couples between potentials of -0.2 and 1.0 V, with the formal potentials being at about 0.06, 0.26, 0.72, and 0.92 V (vs. Ag|AgCl ; see Fig. 6A). Figure 6B shows the EQCM frequency change recorded during the first ten cycles of the consecu-

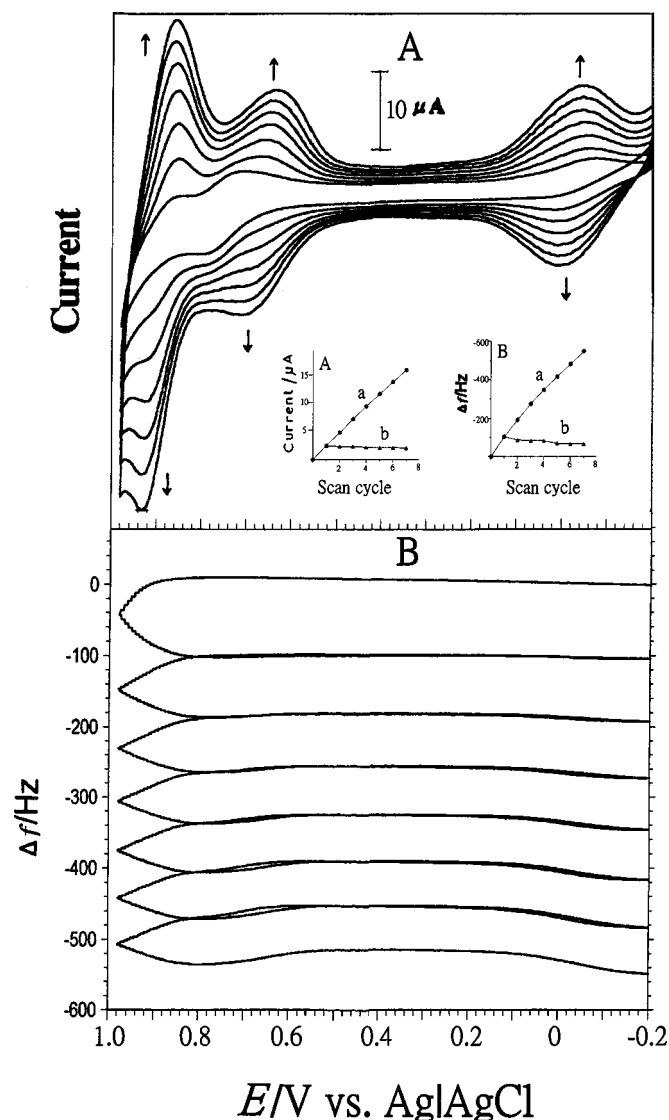


Figure 5. (A) Consecutive CVs of a gold electrode modified with an RP film synthesized from 1×10^{-3} M $\text{Ru}(\text{CN})_6^{4-}$ added to 1×10^{-3} M Ru^{3+} in an aqueous 0.1 M RbNO_3 solution at pH 2.0. Scan rate 0.02 V/s. (B) Change in EQCM frequency recorded concurrently with the consecutive CVs of Fig. 5A. Inset 5A: Plot of (a) cathodic peak current vs. scan cycle at a potential of -0.04 V and (b) change in cathodic peak current during a single scan cycle vs. scan cycle. Inset 5B: Plot of (a) total frequency change vs. scan cycle and (b) frequency change over a single scan cycle vs. scan cycle.

tive CV. The voltammetric peak current in Fig. 6A and the frequency decrease (or mass increase) in Fig. 6B are consistent with the growth of the RP and mvRuO/RuCN hybrid film on the gold electrode. The EQCM results show that the deposition of the film obviously occurred between two potential ranges: one between 0.85 and 1.0 V (vs. Ag|AgCl) and the second between 0.2 and -0.2 V (vs. Ag|AgCl). During the first CV scan, about 1300 ng/cm^2 of RP and mvRuO/RuCN hybrid film was deposited on the gold electrode, and a total of about 9800 ng/cm^2 of RP and mvRuO/RuCN hybrid film was deposited on the gold electrode after ten CV scans. The EQCM data in Fig. 4-6 were also used to estimate the RP and mvRuO/RuCN deposition on the gold electrode for the RP and mvRuO/RuCN hybrid film. The mass of RP and mvRuO/RuCN hybrid film on the gold electrode surface was estimated to be about 5800 ng/cm^2 of mvRuO/RuCN and about 4000 ng/cm^2 of RP.

EQCM measurements are a very good method for monitoring the *in situ* growth of RP, mvRuO/RuCN, and RP and mvRuO/RuCN

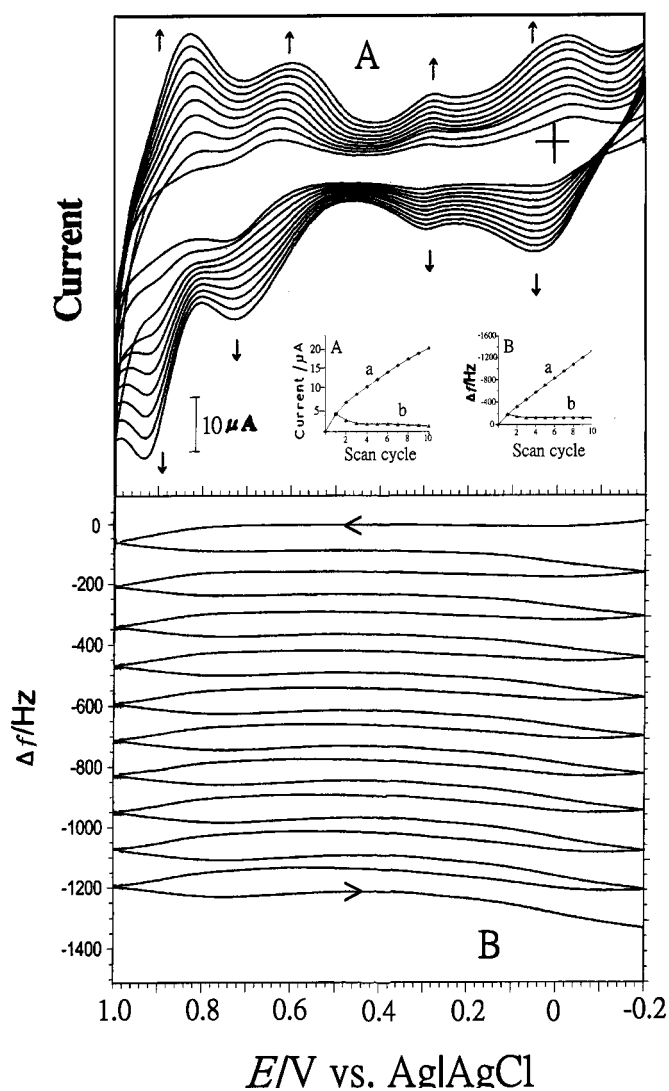


Figure 6. (A) Consecutive CVs of a gold electrode modified with a ruthenium oxide/ruthenocyanide film synthesized from 1×10^{-3} M Ru^{3+} , 1×10^{-3} M Fe^{3+} , and 2×10^{-3} M $\text{Ru}(\text{CN})_6^{4-}$ in an aqueous 0.1 M RbNO_3 solution at pH 2.0. Scan rate 0.02 V/s. (B) Change in EQCM frequency recorded concurrently with the consecutive CVs of Fig. 6A. Inset 6A: Plot of (a) cathodic peak current vs. scan cycle at a potential of 0.0 V and (b) change in cathodic peak current over a single scan cycle vs. scan cycle. Inset 6B: Plot of (a) total frequency change vs. scan cycle and (b) frequency change over a single scan cycle vs. scan cycle.

hybrid films on gold electrodes, and these films all grow steadily vs. time on a gold electrode. The EQCM measurements obviously show that the deposition of the RP film occurred at a potential more negative than 0.2 V (see Fig. 4B) and that the deposition potential of the mvRuO/RuCN film occurred at potentials more positive than 0.85 V (vs. Ag|AgCl) (see Fig. 5B). The deposition potential of the RP and mvRuO/RuCN hybrid film occurred over two potential ranges: one more positive than 0.85 V (vs. Ag|AgCl), and the other more negative than 0.2 V (vs. Ag|AgCl). The results also show that the RP and mvRuO/RuCN hybrid film, which exhibits four redox couples and two deposition potential ranges, shows similar behavior to that of combined RP and mvRuO/RuCN films.

The single redox couple of RP is attributed to the $[\text{Fe}(\text{III})\text{-NC-Ru}(\text{II})]/[\text{Fe}(\text{II})\text{-NC-Ru}(\text{II})]$ redox reaction. There are three redox couples of the mvRuO/RuCN film, which are proposed to arise from the $[\text{Ru}^{\text{II}}\text{-O}]/[\text{Ru}^{\text{II}}(\text{CN})_6]/[\text{Ru}^{\text{III}}\text{-O}]/[\text{Ru}^{\text{II}}(\text{CN})_6]$, $[\text{Ru}^{\text{III}}\text{-O}]/[\text{Ru}^{\text{II}}(\text{CN})_6]/[\text{Ru}^{\text{III}}\text{-O}]/[\text{Ru}^{\text{III}}(\text{CN})_6]$, and

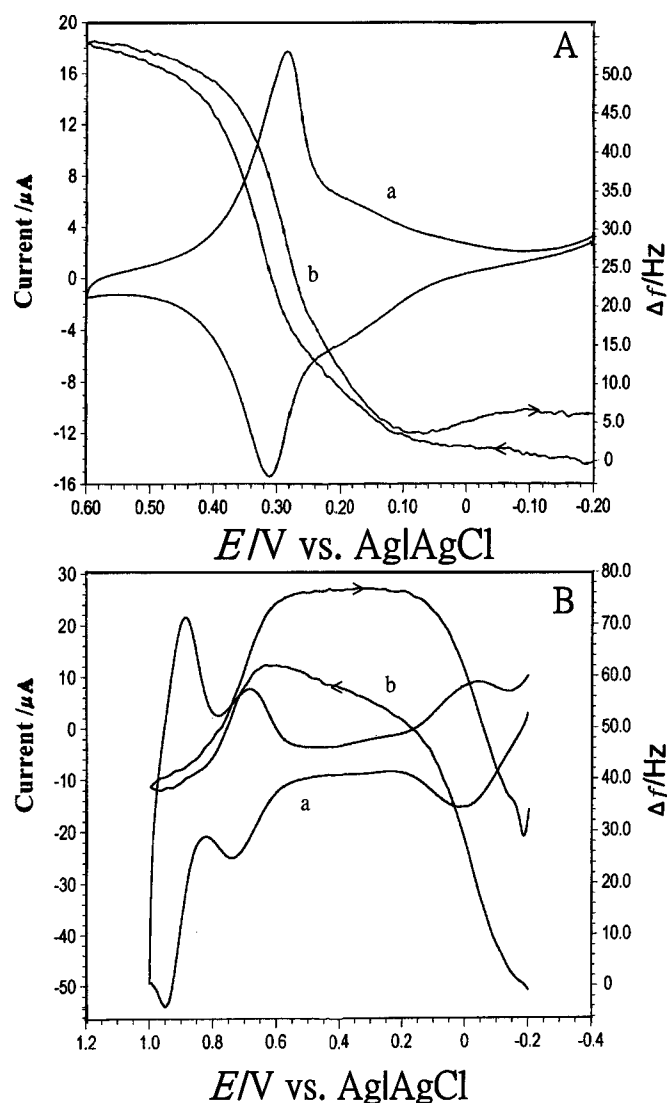


Figure 7. (A,a) CVs of a gold electrode modified with an RP film in an aqueous 0.1 M RbNO_3 solution. (A,b) EQCM frequency change recorded for this film in an aqueous 0.1 M RbNO_3 solution. (B,a) CVs of a gold electrode modified with a ruthenium oxide/ruthenocyanide film in an aqueous 0.1 M RbNO_3 solution. (B,b) EQCM frequency change recorded for this film in an aqueous 0.1 M RbNO_3 solution.

$[\text{Ru}^{\text{III}}\text{-O}]/[\text{Ru}^{\text{III}}(\text{CN})_6]/[\text{Ru}^{\text{IV}}\text{-O}]/[\text{Ru}^{\text{III}}(\text{CN})_6]$ redox processes.

The electrochemical properties of RP and mvRuO/RuCN hybrid films.—Figure 7A shows the CV and EQCM measurements on an RP film in an aqueous 0.1 M RbNO_3 solution. EQCM and potential scanning measurements of an RP film in an aqueous RbNO_3 solution at pH 2.0 were also performed. The EQCM frequency change was recorded during a single cycle using CV between potentials of -0.2 and 0.6 V. The CV frequency (and EQCM) responses recorded during one cycle of the RP film using CV in an RbNO_3 aqueous solution are shown in Fig. 7A. The redox couple voltammetric current varied between potentials of -0.2 and 1.0 V, and the frequency increased/decreased (or mass decreased/increased) with the cation exchange of the single redox couple reaction.

Results showing the single redox couple with voltammetric current (and the frequency change) from potentials of -0.2 to 0.6 V indicating the frequency increase/mass decrease are given in Fig. 7A(a) and 7A(b). The frequency increase (mass decrease) in Fig.

7A(b) is consistent with an Rb^+ ion exchange of the redox couple reaction (from potentials of -0.2 to 0.6 V).

The redox process of RP in Rb^+ and Cs^+ electrolyte aqueous solutions may be written as follows^{15,32-34}

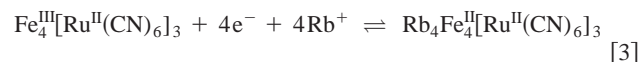


Figure 7B shows the results of the CV and EQCM measurements of an mvRuO/RuCN film in an aqueous 0.2 M RbNO_3 solution at pH 2.0. EQCM and potential scanning measurements of an mvRuO/RuCN film in an aqueous 0.2 M RbNO_3 solution at pH 2.0 were also performed. The EQCM frequency change was recorded over a single cycle using CV between potentials of -0.2 and 1.0 V. The CV frequency (or EQCM) responses recorded during a single cycle using CV in an aqueous RbNO_3 solution are shown in Fig. 7B(a) and 7B(b). The redox couple voltammetric current varied between potentials of -0.2 and 1.0 V, and the frequency increased/decreased (or mass decreased/increased) with the cation exchange of the three redox couple reactions.

The results showing the three redox couples with voltammetric currents (and the frequency change) from potentials of -0.2 to 0.4 V (frequency increase/mass decrease), from potentials of 0.40 to $+0.85$ V (frequency decrease/mass increase), and from potentials of 0.85 to 1.0 V (no obvious change in frequency) are given in Fig. 7B(b). The frequency increase (mass decrease) in Fig. 7B(b) is consistent with an Rb^+ ion exchange of the redox couple reaction from potentials of -0.2 to 0.4 V. The frequency decrease/mass increase in Fig. 7B(b) is consistent with an Rb^+ ion exchange of the redox couple reaction from potentials of 0.40 – 0.85 V, and with the frequency showing no obvious change from potentials of 0.85 – 1.0 V.

Figure 8 shows the results of CV and EQCM measurements of an RP and mvRuO/RuCN hybrid film in an aqueous 0.2 M RbNO_3 solution at pH 2.0. EQCM and potential scanning measurements of a hybrid RP and mvRuO/RuCN film in an aqueous RbNO_3 solution were also performed. The EQCM frequency change was recorded over a single cycle using CV between potentials of -0.2 and 1.0 V. The CV frequency (or EQCM) responses recorded for the hybrid RP and mvRuO/RuCN film during a single cycle using CV in an aqueous RbNO_3 solution are shown in Fig. 8A(a) and 8A(b). The redox couple voltammetric current varied between potentials of -0.2 and 1.0 V, and the frequency increased/decreased (or mass decreased/increased) with the cation exchange of the three redox couple reactions.

Results showing the four redox couples with voltammetric currents (and frequency change) in potential ranges of -0.2 to 0.2 V (frequency increase/mass decrease), 0.2 – 0.5 V (frequency increase/mass decrease), 0.5 – 0.85 V (frequency decrease/mass increase), and in the potential range 0.85 – 1.0 V (no obvious change in frequency) are given in Fig. 8A. The frequency increase (or mass decrease) in Fig. 8A is consistent with an Rb^+ ion exchange of the two redox couples (in the potential ranges of -0.2 to 0.2 and 0.2 – 0.5 V). The frequency decrease (or mass increase) in Fig. 8A is consistent with an Rb^+ ion exchange of the redox couple in the potential range 0.50 – 0.85 V, and with no obvious change in frequency in the potential range 0.85 – 1.0 V.

Kinetics of potential switching in the potential range of -0.2 to 0.2 V [Fig. 8B(a)], 0.2 – 0.5 V [Fig. 8B(b)], and 0.5 – 0.85 V [Fig. 8B(c)] were elucidated to assess the performance of a hybrid RP and mvRuO/RuCN film in RbNO_3 in these experiments. A square wave potential was applied over a 2 s period during film cation exchange. The results are shown in Fig. 8B. The reversibility of the hybrid RP and mvRuO/RuCN film during the cycling and frequency change was good, and cation exchange is obvious from the redox couples. From the EQCM results, the kinetics of the cation exchange rate in

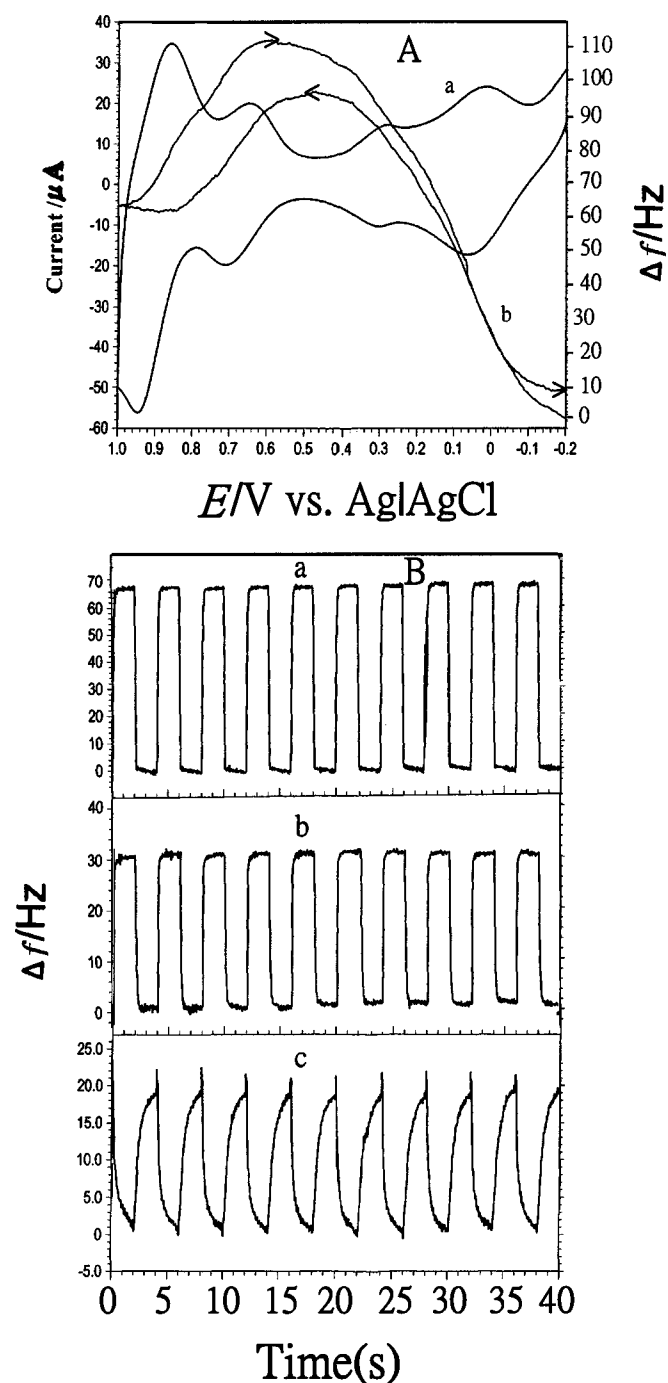


Figure 8. (A,a) CVs of a gold electrode modified with an RP and mvRuO/RuCN hybrid film in an aqueous 0.1 M RbNO₃ solution. (A,b) EQCM frequency change recorded for this film in an aqueous 0.1 M RbNO₃ solution. (B) EQCM measurements on an RP and mvRuO/RuCN hybrid film in an aqueous 0.1 M RbNO₃ solution during potential switching from (a) $E_{\text{appl}} = -0.2$ to 0.2 V vs. Ag|AgCl, (b) $E_{\text{appl}} = 0.2$ -0.45 V vs. Ag|AgCl, and (c) $E_{\text{appl}} = 0.45$ -0.8 V vs. Ag|AgCl with 2 s time pulses.

the potential ranges of -0.2 to 0.2 V [Fig. 8B(a)] and 0.2 - 0.5 V [Fig. 8B(b)] were both faster than the cation exchange rate in the potential range of 0.5 - 0.85 V [Fig. 8B(c)].

For a one-electron redox couple, $n = 1$, the effective molar mass, M , was estimated to be about 2290 g/mol. Figure 7A shows the EQCM results of a 9450 ng/cm² (about 4.1×10^{-9} mol/cm²) RP film that was deposited on a gold electrode (if one effective

molar mass is taken to be equivalent to 1 mol of positive charge exchanged, *i.e.*, 1 mol of Rb⁺).

The EQCM results in Fig. 7A show that an increase in frequency (or a decrease in mass) had occurred during the oxidation of the mvRuO/RuCN film. During the CV, the frequency change was about 18.4 Hz (or 25.8 ng) for a 0.196 cm² gold electrode. This frequency change was smaller than that of the frequency exchange occurring at the film (if the total Rb⁺ ion exchange reaction in the film that had a frequency change of about 50 Hz). These results show that there was perhaps water (solvent) transfer in the switching of the RP film, as water would exit an RP film upon cation insertion. The EQCM results of ruthenium oxide/hexacyanoruthenate films also exhibit a similar phenomenon.

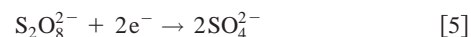
Figure 6B and 8 show the EQCM results of a 9800 ng/cm² (1.1×10^{-9} mol/cm²) ruthenium oxide/hexacyanoruthenate and RP hybrid film that was deposited on a gold electrode. For a one-electron redox couple, $n = 1$, the effective molar mass, M , was estimated to be about 1840 g/mol at the peak potential of 0 V (assuming that one effective molar mass is taken to be equivalent to 1 mol positive charge, *i.e.*, 1 mole of Rb⁺, exchanged).

The EQCM results in Fig. 8B show that an increase in frequency (or a decrease in mass) had occurred during the oxidation of the ruthenium oxide/hexacyanoruthenate and RP hybrid film. During the CV, the frequency change was about 67 Hz (or 93.8 ng) for a 0.196 cm² gold electrode (assuming that the total Rb⁺ ion-exchange reaction had a frequency change of about 19 Hz). This frequency change was larger than that of the frequency exchange occurring at the film. These results also show that there was perhaps water (solvent, or hydrated ion) transfer occurring during the switching of the film, as water (or hydrated ions) would be exchanged in the hybrid film upon cation insertion.

Electrocatalytic reduction of S₂O₈²⁻ and SO₅²⁻ by hybrid ruthenium(III) ruthenocyanide and RP films.—The electrocatalytic reduction of S₂O₈²⁻ and SO₅²⁻ by hybrid RP and mvRuO/RuCN films in aqueous 0.2 M RbNO₃ solutions at pH 2.0 was investigated.

Figure 9A shows the CVs of the hybrid RP and mvRuO/RuCN film in an aqueous 0.2 M RbNO₃ buffered solution at pH 2.0 in the absence and presence of S₂O₈²⁻. The cathodic peak current of the hybrid RP and mvRuO/RuCN film for the redox couple at 0.05 V (*vs.* Ag|AgCl) increased noticeably, while the anodic peak current decreased as the concentration of S₂O₈²⁻ increased. The cathodic peak current of the hybrid RP and mvRuO/RuCN film redox couple at 0.30 V (*vs.* Ag|AgCl) also increased, but a smaller electrocatalytic current was observed. The experimental results also show the CVs of a hybrid RP and mvRuO/RuCN film in an aqueous 0.2 M RbNO₃ buffered solution at pH 2.0 in the presence of SO₅²⁻. An increase in the cathodic peak current appears as the concentration of SO₅²⁻ increases in the aqueous 0.2 M RbNO₃ solution at pH 2.0. Figure 9B shows the CVs of a hybrid RP and mvRuO/RuCN film in an aqueous 0.2 M RbNO₃ buffered solution at pH 2.0 in the absence and presence of SO₅²⁻. The cathodic peak current of the two redox couples of the hybrid RP and mvRuO/RuCN film at potentials of about 0.05 and 0.30 V (*vs.* Ag|AgCl) both increased noticeably, but the other two redox couples of the hybrid RP and mvRuO/RuCN film that occurred at potentials between 0.6 and 1.1 V (*vs.* Ag|AgCl) stayed the same and showed no obvious electrocatalytic current. In aqueous solutions of the cesium or rubidium electrolytes, the electrocatalytic processes that developed from the redox couples were easier to observe than in the corresponding potassium or sodium aqueous electrolyte solutions.

The electrocatalytic activity was shown only through the two negative redox couples of the hybrid RP and mvRuO/RuCN film.



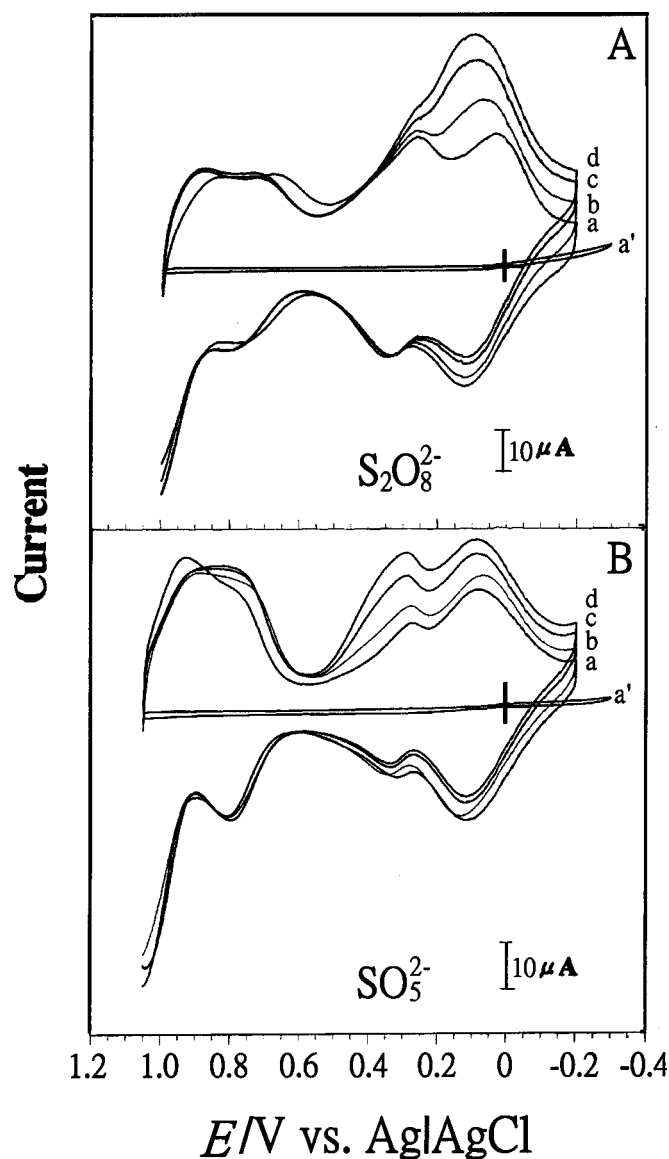


Figure 9. (A) CVs of a hybrid ruthenium(III) ruthenocyanide and iron(III) ruthenocyanide film adhered to a GC electrode in a 0.1 M RbNO₃ solution at pH 2.0. (A) [SO₅²⁻] = (a) 0.0, (b) 5 × 10⁻³, (c) 1.0 × 10⁻², and (d) 2.0 × 10⁻² M. (a') Bare GC electrode, [SO₅²⁻] = 2.0 × 10⁻² M. (B) [S₂O₈²⁻] = (a) 0.0, (b) 6 × 10⁻³, (c) 1.2 × 10⁻², and (d) 2.4 × 10⁻² M. (a') Bare GC electrode, [S₂O₈²⁻] = 2.4 × 10⁻² M.

Electrocatalysis of dopamine and epinephrine by hybrid RP and mvRuO/RuCN films.—The electrocatalytic oxidation of dopamine and epinephrine by a hybrid RP and mvRuO/RuCN film in an aqueous 0.2 M RbNO₃ solution at pH 5.0 was investigated. Figure 10A shows the CVs of a hybrid RP and mvRuO/RuCN film in an aqueous 0.2 M RbNO₃ buffered solution at pH 5.0 in the absence and presence of dopamine. The anodic peak current of the hybrid RP and mvRuO/RuCN film of the redox couple at a potential of about 0.30 V (vs. Ag|AgCl) increased noticeably, and the cathodic peak current also increased, as the concentration of dopamine increased. The cathodic peak current of the hybrid RP and mvRuO/RuCN film redox couple at a potential of about 0.0 V (vs. Ag|AgCl) showed no electrocatalytic current. Figure 10B shows the CVs of a hybrid RP and mvRuO/RuCN film in an aqueous 0.2 M RbNO₃ buffered solution at pH 5.0 in the absence and presence of epinephrine. The anodic peak current of the redox couple of the hybrid RP and mvRuO/RuCN film at a potential of about 0.30 V (vs. Ag|AgCl) increased

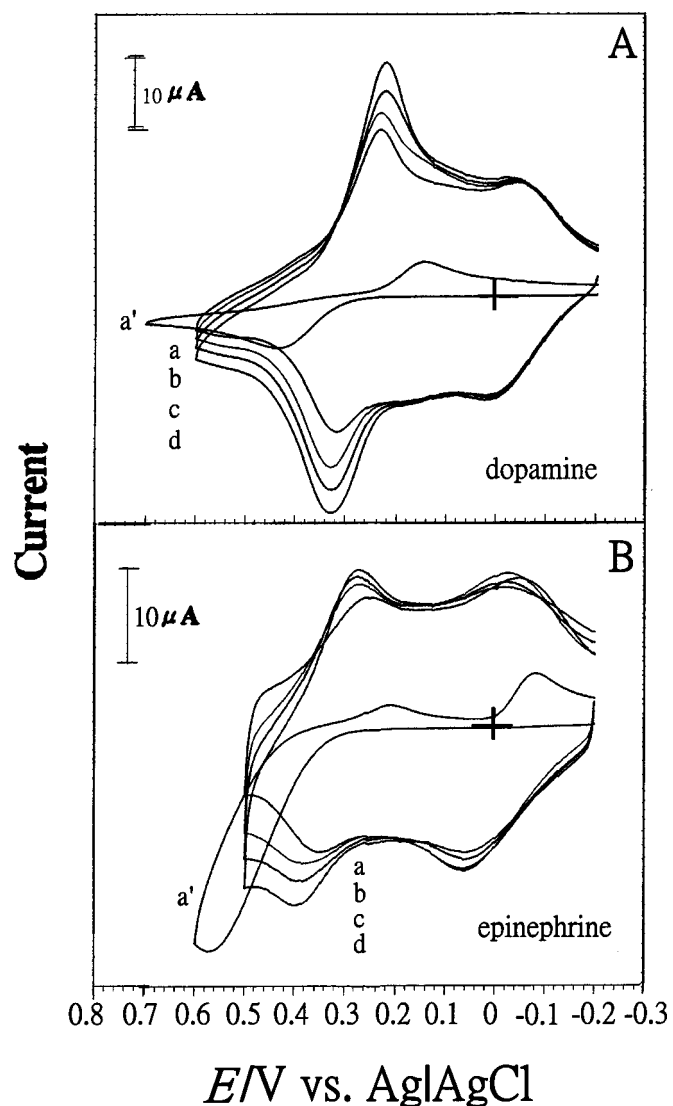


Figure 10. (A) CVs of a hybrid ruthenium(III) ruthenocyanide and iron(III) ruthenocyanide film adhered to a GC electrode in a 0.1 M RbNO₃ solution at pH 5.0. (A) [dopamine] = (a) 0.0, (b) 4 × 10⁻³, (c) 7 × 10⁻³, and (d) 1 × 10⁻² M. (a') Bare GC carbon electrode, [dopamine] = 1 × 10⁻² M. (B) [epinephrine] = (a) 0.0, (b) 4 × 10⁻³, (c) 7 × 10⁻³, and (d) 1 × 10⁻² M. (a') Bare GC electrode, [epinephrine] = 1 × 10⁻² M.

noticeably, and an increasing cathodic peak current (electrocatalytic reduction) appeared as the concentration of epinephrine increased. The other redox couple of the hybrid RP and mvRuO/RuCN film at a potential of about 0.0 V (vs. Ag|AgCl) showed no obvious electrocatalytic current.

Both the anodic and cathodic peak currents increased as the concentration of dopamine (or epinephrine) increased. The electrocatalytic oxidation of dopamine (or epinephrine) and the reduction of its oxidation products were both electrocatalytically active when using a hybrid RP and mvRuO/RuCN film in an aqueous solution at pH 5.0 (see Table II).

Electrocatalytic oxidation of dopamine by a hybrid RP and mvRuO/RuCN film in an aqueous solution at pH 5.0 is described by the following reaction scheme³⁷⁻³⁹

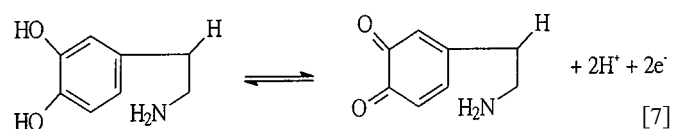


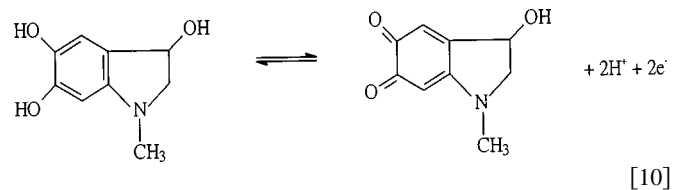
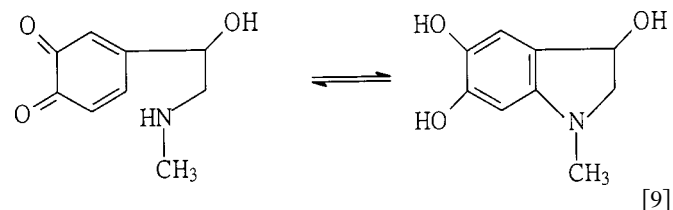
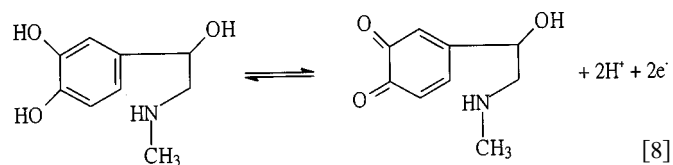
Table II. The electrocatalytic properties of dopamine with a hybrid RP and mvRuO/RuCN film and a bare GC electrode in aqueous solutions at pH 5.0.

Electrode ^a	Anodic peak potential (V)	Cathodic peak potential (V)	ΔE_p (V)	Reactant ^b
RP and mvRuO/RuCN	0.33	0.22	0.11	Dopamine
GC	0.44	0.13	0.31	Dopamine
RP and mvRuO/RuCN	0.38	0.27	0.11	Epinephrine
GC	0.56	0.21	0.35	Epinephrine

^a GC is a bare glassy carbon electrode.

^b The first cathodic peak potential.

The electrocatalytic oxidation of epinephrine by a hybrid ruthenium(III) ruthenocyanide and RP film in an aqueous solution at pH 5.0 is described by³⁷⁻³⁹



The CVs of epinephrine in an aqueous buffered solution at pH 5.0 shows one oxidation peak and two reduction peaks (Fig. 10B). The irreversible oxidation peak occurred at a potential of about 0.57 V (vs. Ag|AgCl) and stems from the oxidation reaction shown in Eq. 8-10. The two reduction peaks occurring at potentials of about 0.22 and -0.08 V (vs. Ag|AgCl) arise from the reduction reactions shown in Eq. 8 and 10.

Study of the electrocatalytic oxidation properties using the RRDE method.—Figure 11 shows the electrocatalytic oxidation of dopamine by a hybrid RP and mvRuO/RuCN film using the RRDE method. Figure 11A shows the dopamine present in an aqueous solution at pH 5.0 with different concentrations of dopamine when the hybrid RP and mvRuO/RuCN film modified ring GC electrode had an applied potential of 0.1 V (vs. Ag|AgCl) at 2500 rpm. Figure 11B shows the dopamine present in an aqueous solution at pH 5.0 when the hybrid RP and mvRuO/RuCN film modified ring GC electrode had an applied potential of 0.1 V (vs. Ag|AgCl) and [dopamine] = 4×10^{-4} M for different rotation rates. The inset of Fig. 11A shows a plot of I_D and I_{cat} (I_D minus the disk current in the absence of dopamine) and I_R vs. [dopamine], illustrating a close linear dependence of I_D , I_{cat} , and I_R on the scan rate. The values of I_D and I_R are the oxidation and reduction currents at 0.37 (Fig. 11) and 0.42 V (Fig. 12), respectively (where I_D reaches a plateau). The ratio of $I_R:I_D$ was equal to 0.30, and the collection efficiency, N , is defined as I_R/I_D .

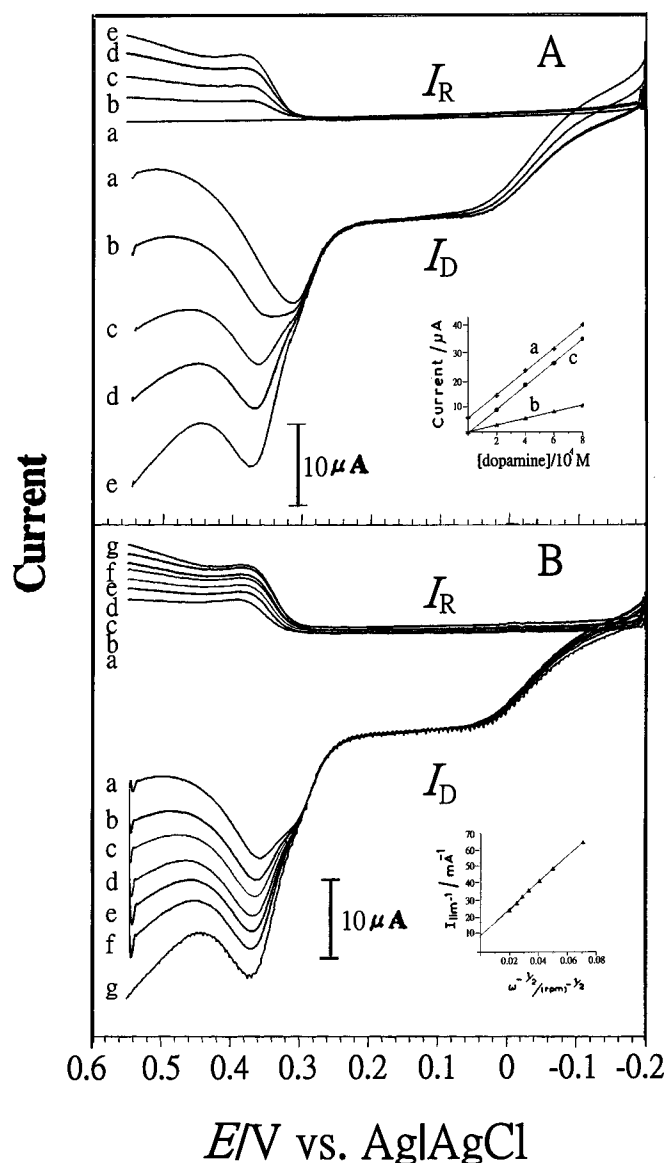


Figure 11. (A) RRDE voltammogram of a hybrid ruthenium(III) ruthenocyanide and iron(III) ruthenocyanide film adsorbed on a GC electrode with differing concentrations of dopamine in an aqueous 0.1 M RbNO₃ solution at pH 5.0. [dopamine] = (a) 0.0, (b) 2×10^{-4} , (c) 4×10^{-4} , (d) 6×10^{-4} , and (e) 8×10^{-4} M at a rotation rate of 2500 rpm. $E_R = 0.15$ V. Inset 11A: Plot of (a) I_R , (b) I_D , and (c) I_{cat} vs. [dopamine]. (B) RRDE voltammogram of a hybrid ruthenium(III) ruthenocyanide and iron(III) ruthenocyanide film adsorbed on a GC disk electrode in an aqueous 0.1 M RbNO₃ solution at pH 5.0 with different rotation rates: (a) 200, (b) 400, (c) 600, (d) 900, (e) 1200, (f) 1600, and (g) 2500 rpm. [dopamine] = 4×10^{-4} M. $E_R = 0.15$ V. Inset 11B: Plot of I^{-1} vs. $\omega^{-1/2}$.

In Fig. 11B, the value of I_D is the oxidation current and the value of I_R is the reduction current shown in Eq. 7. The collection efficiency for various rotating rates plotted as I_R/I_D vs. $\omega^{1/2}$ was almost constant, with an average value close to 0.25 (for $E_R = 0.1$ V). These results are consistent with the current I_R being the reduction current shown in Eq. 7. The RRDE data were analyzed using the Koutecky-Levich equation^{30,40,41} and plotted as I^{-1} vs. $\omega^{-1/2}$, as shown in the inset of Fig. 11B

$$1/I = 1/I_k + 1/I_{\text{lim},c} \quad [11]$$

where

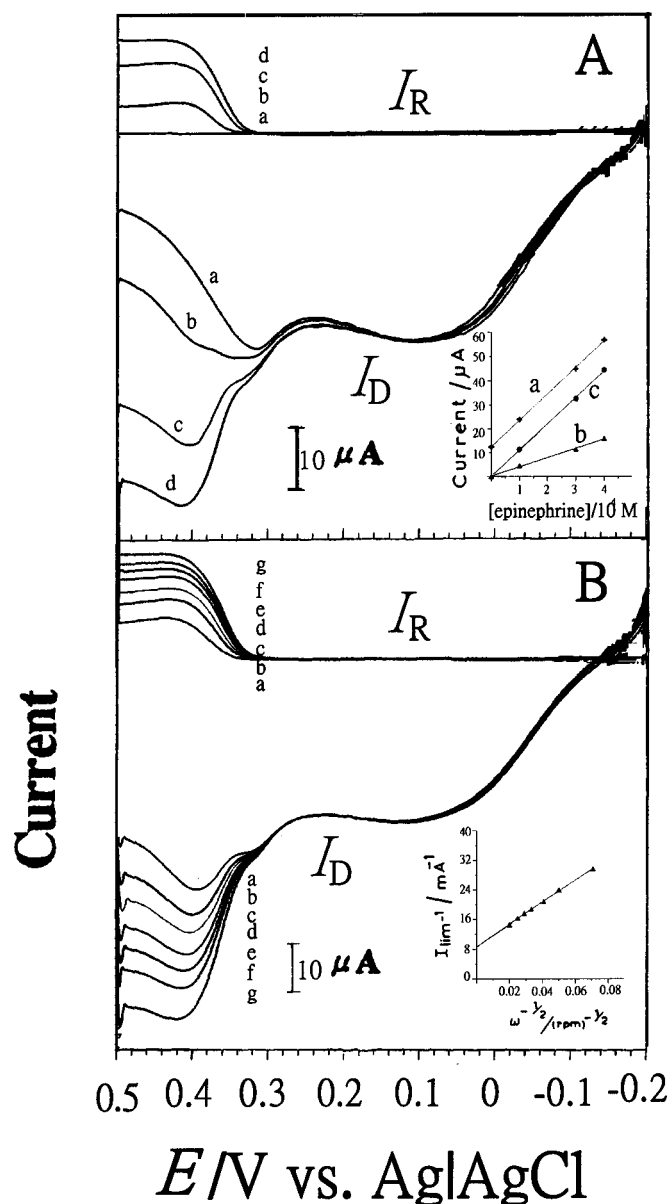


Figure 12. (A) RRDE voltammogram of a hybrid ruthenium(III) ruthenocyanide and iron(III) ruthenocyanide film adsorbed on a GC disk electrode with differing concentrations of epinephrine in an aqueous 0.1 M RbNO₃ solution at pH 5.0. [epinephrine] = (a) 0.0, (b) 1×10^{-4} , (c) 3×10^{-4} , and (d) 4×10^{-4} M at a rotation rate of 2500 rpm. $E_R = 0.15$ V. Inset 12A: Plot of (a) I_R , (b) I_D , and (c) I_{cat} vs. [epinephrine] at 0.38 V. (B) RRDE voltammogram of a hybrid ruthenium(III) ruthenocyanide and iron(III) ruthenocyanide film adsorbed on a GC disk electrode in an aqueous 0.1 M RbNO₃ solution at pH 4.0 with different rotation rates: (a) 200, (b) 400, (c) 600, (d) 900, (e) 1200, (f) 1600, and (g) 2500 rpm. [epinephrine] = 4×10^{-4} M. $E_R = -0.2$ V. Inset 12B: Plot of I^{-1} vs. $\omega^{-1/2}$.

$$I_{lim,c} = 0.62nFAD_0^{2/3}\omega^{1/2}\nu^{-1/6}C_0^* \quad [12]$$

The parameter $I_{lim,c}$ is the measured limiting current of the disk, ω is the rotation rate, D_0 and C_0^* are the diffusion coefficient and the bulk concentration of dopamine, respectively, and ν is the kinematic viscosity of water in the experimental rotating rates. In Fig. 11 and 12, the zero current is observed at a potential of about -0.15 V, and the values of I_D and I_R are the oxidation and reduction currents at potentials of 0.37 (Fig. 11) and 0.42 V (Fig. 12), respectively (where the value of I_D reaches a plateau). The baseline zero current was at

a potential of about -0.15 V for I_D and I_R . The best straight line passing through the data points was then selected and the RRDE data analyzed using the Koutecky-Levich equation and plotted as I^{-1} vs. $\omega^{-1/2}$, as shown in the insets of Fig. 11B and 12B.

The inset of Fig. 11B shows a plot of I^{-1} vs. $\omega^{-1/2}$, for $I_k = nFAk\Gamma C_0^*$, where k is the rate constant of the chemical reaction between the film and dopamine, and Γ is the coverage of the catalyst on the electrode surface. Γ was estimated to be 7.8×10^{-8} mol/cm² for the RP film, and the rate constant was estimated to be 5.2×10^2 M⁻¹ s⁻¹.

Figure 12 shows the electrocatalytic oxidation of epinephrine by a hybrid RP and mvRuO/RuCN film using the RRDE method. Figure 12A shows the epinephrine present in an aqueous solution at pH 5.0 when the hybrid RP and mvRuO/RuCN film modified ring GC electrode had an applied potential of 0.1 V (vs. Ag|AgCl) with different concentrations of epinephrine at 2500 rpm. The inset of Fig. 12A shows a plot of I_D , I_{cat} (I_{cat} is $I_{D,lim}$ minus the disk current when the reactant concentration is zero at the same potential in the presence of catalytic film), and I_R vs. [epinephrine], respectively, illustrating a close linear dependence of I_D , I_{cat} , and I_R on the scan rate, and that $I_R:I_D$ was equal to 0.30.

Figure 12B shows the oxidation of epinephrine present in a pH 5.0 buffered solution when a ring GC electrode potential was applied at -0.2 V (vs. Ag|AgCl) at different rotation rates. The parameter I_D is the oxidation current shown in Eq. 8 and of the further oxidation shown in Eq. 10. In Fig. 12B, I_R denotes the reduction current of Eq. 8 and 10. The RRDE data were also analyzed using the Koutecky-Levich equation^{40,41} ($1/I = 1/I_k + 1/I_{lim,c}$), where $I_{lim,c}$ is the observed limiting current of the disk and $I_k = nFA\kappa\Gamma$ [epinephrine]. Plots of I^{-1} vs. $\omega^{-1/2}$ are shown in the inset of Fig. 12B. The surface coverage, Γ , was estimated to be 8×10^{-8} mol/cm² for the RP in the hybrid film, as deduced from the chronocoulometry charge and the EQCM frequency. The rate constant of the chemical reaction, κ , was estimated to be an average value of 5.0×10^2 M⁻¹ s⁻¹ from three epinephrine concentrations: 1×10^{-4} , 2×10^{-4} , and 4×10^{-4} M.

The electrocatalytic properties depicted in Fig. 11 and 12 clearly show the electrochemical oxidation and electrocatalytic reduction of dopamine and epinephrine and their oxidation products by a hybrid RP and mvRuO/RuCN film.

Conclusions

Hybrid RP and mvRuO/RuCN films were successfully synthesized using consecutive CV on various electrodes directly from Ru³⁺, Fe³⁺, and Ru(CN)₆⁴⁻ ions in various electrolyte solutions containing Rb⁺ and Cs⁺ cations. The formal potentials and shapes of the CVs show four obvious and separated redox couples which depended on the electrolyte cation.

EQCM and CV were used to study the growth mechanisms of the RP and mvRuO/RuCN films, and the hybrid RP and mvRuO/RuCN films. EQCM and CV were used to study the *in situ* growth of the RP, mvRuO/RuCN, and hybrid RP and mvRuO/RuCN films. The results indicate that the redox processes were confined to the surface, confirming the immobilized state of the RP and mvRuO/RuCN, and the hybrid RP and mvRuO/RuCN films. The ionic exchange processes of the RP, mvRuO/RuCN, and the hybrid RP and mvRuO/RuCN films were also discussed using EQCM and CV.

The hybrid RP and mvRuO/RuCN films can electrocatalytically reduce SO₅²⁻ and S₂O₈²⁻. Hybrid RP and mvRuO/RuCN films are electrocatalytically active in the oxidation of dopamine and epinephrine. The electrocatalytic reactions of dopamine and epinephrine with hybrid RP and mvRuO/RuCN films were investigated using the RRDE method and the rate constant of the chemical reaction was estimated.

Acknowledgment

This work was supported by the National Science Council of the Republic of China.

The National Taipei University of Technology assisted in meeting the publication costs of this article.

References

1. K. Itaya, I. Uchida, and V. D. Neff, *Acc. Chem. Res.*, **19**, 162 (1986).
2. V. D. Neff, *J. Electrochem. Soc.*, **132**, 1382 (1985).
3. K. Honda and H. Hayashi, *J. Electrochem. Soc.*, **134**, 1330 (1987).
4. T. R. I. Cataldi and G. E. De Benedetto, *J. Electroanal. Chem.*, **458**, 149 (1998).
5. L. M. Siperko and T. Kuwana, *J. Electrochem. Soc.*, **130**, 396 (1983).
6. D. N. Upadhyay and D. M. Kolb, *J. Electroanal. Chem.*, **358**, 317 (1993).
7. B. D. Humphrey, S. Sinha, and A. B. Bocarsly, *J. Phys. Chem.*, **91**, 586 (1987).
8. J. A. Cox and P. J. Kulesza, *Anal. Chem.*, **56**, 1021 (1984).
9. K. Ogura and I. Yoshida, *Electrochim. Acta*, **32**, 1191 (1987).
10. C. Lin and A. B. Bocarsly, *J. Electroanal. Chem.*, **300**, 325 (1991).
11. P. J. Kulesza, K. Brajter, and E. Dabek-Zlotorzynska, *Anal. Chem.*, **59**, 2776 (1987).
12. S.-M. Chen, *J. Electroanal. Chem.*, **521**, 29 (2002).
13. S.-M. Chen, *J. Electroanal. Chem.*, **401**, 147 (1996).
14. S.-M. Chen, *Electrochim. Acta*, **43**, 3359 (1998).
15. S.-M. Chen and S.-H. Hsueh, *J. Electrochem. Soc.*, **150**, D175 (2003).
16. R. J. Mortimer and D. R. Rosseinsky, *J. Chem. Soc. Dalton Trans.*, **1984**, 2059.
17. K. Tanaka and R. Tamamushi, *J. Electroanal. Chem.*, **380**, 279 (1995).
18. H. Kahlert, U. Retter, H. Lohse, K. Siegler, and F. Scholz, *J. Phys. Chem.*, **102**, 8757 (1998).
19. L. T. Kubota and Y. Gushikem, *J. Electroanal. Chem.*, **362**, 219 (1993).
20. K. P. Rajan and V. D. Neff, *J. Phys. Chem.*, **86**, 4361 (1982).
21. K. Itaya, T. Ataka, and S. Toshima, *J. Am. Chem. Soc.*, **104**, 3751 (1982).
22. F. C. Crean and K. Schug, *Inorg. Chem.*, **23**, 853 (1984).
23. J. A. Cox and T. Gray, *Anal. Chem.*, **61**, 2462 (1989).
24. W. Gorski and J. A. Cox, *J. Electroanal. Chem.*, **389**, 123 (1995).
25. T. R. I. Cataldi, D. Centonze, E. Desimoni, and V. Forastiero, *Anal. Chim. Acta*, **310**, 257 (1995).
26. R. T. Kennedy, L. Huang, M. A. Atkinson, and P. Dush, *Anal. Chem.*, **65**, 1882 (1993).
27. J. A. Cox and K. Lewinski, *Electroanalysis*, **6**, 976 (1994).
28. C.-F. Chen and C.-M. Wang, *J. Electroanal. Chem.*, **466**, 82 (1999).
29. T. R. I. Cataldi, G. E. de Benedetto, and C. Campa, *J. Electroanal. Chem.*, **437**, 93 (1997).
30. A. J. Bard and L. R. Faulkner, *Electrochemical Methods Fundamentals and Applications*, John Wiley & Sons, New York (1980).
31. A. P. Brown and F. C. Anson, *Anal. Chem.*, **49**, 1589 (1977).
32. P. J. Kulesza, *J. Electroanal. Chem. Interfacial Electrochem.*, **220**, 295 (1987).
33. C.-F. Chen and C.-M. Wang, *J. Electroanal. Chem.*, **466**, 82 (1999).
34. T. R. I. Cataldi, G. E. de Benedetto, and C. Campa, *J. Electroanal. Chem.*, **437**, 93 (1997).
35. D. A. Buttry, in *Electroanalytical Chemistry*, Vol. 17, A. J. Bard, Editor, Dekker, New York (1992).
36. S. J. Reddy, A. D. Fritz, and J. Scholz, *J. Electroanal. Chem.*, **403**, 209 (1996).
37. P. Hernandez, I. Sanchez, F. Paton, and L. Hernandez, *Talanta*, **46**, 985 (1998).
38. S.-M. Chen and K.-C. Lin, *J. Electroanal. Chem.*, **523**, 93 (2002).
39. S.-M. Chen and K.-T. Peng, *J. Electroanal. Chem.*, **547**, 179 (2003).
40. A. J. Bard and L. R. Faulkner, *Electrochemical Method Fundamentals and Applications*, Wiley, New York (2001).
41. R. R. Durand, Jr., C. S. Bencosme, J. P. Collman, and F. C. Anson, *J. Am. Chem. Soc.*, **105**, 2710 (1983).